Journal of Applied Polymer Science

Preparation and Evaluation of Nonphosphate Terpolymer as Scale Inhibitor and Dispersant for $Ca_3(PO_4)_2$, $BaSO_4$, and Iron (III) Hydroxide Scales

Yunyun Bu,[1] Yuming Zhou,[1] Qingzhao Yao,[1] Yiyi Chen,[1] Wei Sun,[2] Wendao Wu[2]

[1]School of Chemistry and Chemical Engineering, Southeast University, Nanjing 211189, People's Republic of China

[2]Jianghai Environmental Protection Co., Ltd, Changzhou 213116, Jiangsu, People's Republic of China

Correspondence to: Y. Zhou (E-mail: ymzhou@seu.edu.cn) and Q. Yao (E-mail: 101006377@seu.edu.cn)

ABSTRACT: The polymeric scale inhibition and dispersion agents (PAYS) were prepared by graft copolymerization of acrylic acid, allyl-polyethoxy carboxylate (APEY) and 2-acrylamido-2-methyl-propanesulfonic acid by using ammonium persulfate as a radical initiator in aqueous solution, among which APEY was synthesized in laboratory. Structure of PAYS was characterized by Fourier transform infrared spectroscopy. Experimental data showed that the terpolymer was a high-efficient chelate sorbent, and it exhibited excellent ability for calcium orthophosphate, with approximately 96% efficiency at the dosage of 4 mg/L, as well as high efficiency toward barium sulfate scales nearly 80% inhibition. The effectiveness of PAYS depends on the agent concentration, temperature and the ratio of the reactant. The formation of $Ca_3(PO_4)_2$ and $BaSO_4$ precipitates was characterized by scanning electron microscopy. It appeared that the crystal shape, size, and the morphology of scale changed apparently at the dosage of 4 and 15 mg/L, respectively. In addition, it has good effect on controlling iron (III) scaling. This study was also devoted to the understanding of the action mechanism of these inhibitors in suppressing the crystal nucleus formation and preventing the crystal growth. Based on the contrast experiment of scale formation, the supposing mechanism diagram was also delineated and analyzed in detail. © 2014 Wiley Periodicals, Inc. J. Appl. Polym. Sci. **2015**, *132*, 41546.

KEYWORDS: addition polymerization; adsorption; crystallization; morphology; polyimides

Received 5 June 2014; accepted 22 September 2014

DOI: 10.1002/app.41546

INTRODUCTION

Scale deposition is an obstinate phenomenon when coming across water containing irons of insoluble salts, which will cause derivative problems such as increasing cleaning frequency and the cost of production, reducing the rate of chemical utilization and product quality, equipment corrosion and pipeline clogging.[1–5] The most common sparingly soluble salts are calcium sulfate, calcium carbonate, calcium phosphate, barium sulfate, calcium oxalate, and iron (III) hydroxide scales, etc.[6–8] Among all kinds of scales, the barium sulfate is most difficult to prevent and calcium phosphate is most difficult to handle.[9] Barium sulfate possesses poor chemical solubility and it is difficult to deal with once formed, as a matter of oilfield water most insoluble scale. Owing to small quantity of $BaSO_4$, the precipitation is produced instantly and the phenomenon cannot be noticed easily. Therefore, the use of scale inhibitors for barium sulfate deposition and relevant reports are rare. To avoid the harm of scale deposition on the equipment and reduce the cost of cleaning process, the treatment of circulating cooling water is significant and urgent for industrial production.

From the angle of scaling mechanism, main aspects are as follows: (1) control deposition and fouling crystal growth; (2) control the ionic attraction between metallic cations and anion; and (3) modify the crystal of scale. Adding scale inhibitors can simultaneously achieve the purpose of modifying the crystal and controlling the crystal growth and it is the most economical and effective method.[10–13]

The development of scale inhibitors has experienced from inorganic to organic, from natural to synthesis, from high phosphorus to low phosphorus or nonphosphorus. Phosphorus inhibitors would cause water eutrophication and even toxic. Meanwhile phosphorus inhibitors have a poor depressing ability on salt scales, such as P, S, Ca, Ba, Mg, because it is easily affected by metal ions in water. In recent decades, the use of copolymers in scale inhibition has greatly increased due to the advantages that these materials present over high performance. Scale inhibition copolymers can generally be divided into natural polymers, carboxylic polymers, phosphino polycarboxylic acid polymers and sulfonated polymers.[14] Natural polymer scale

inhibitors, due to the disadvantages of high content of impurity, large amount of dosage, high cost of investment and poor high-temperature resistance, are now rarely used. Functional groups of polycarboxylic acid inhibitor play the role, such as carboxyl group. Unfortunately, they would react with calcium ions to form insoluble calcium-polymer salts due to their low calcium tolerance.[15,16] Phosphino polycarboxylic acid polymers reduce the content of P in a certain extent, but some problems produced of phosphorus inhibitors are still exist. For example, previous studies have reported that EDTMP [ethylene-diamine-tetrakis (methylene-phosphonate)] shows better anti scale effects on calcium sulfate and barium sulfate but restricted application. It's found that phosphonates encounter some reversion so that there will be some orthophosphate and then supposed to form insoluble phosphonate scales.[17] The development of friendly-to-use, effective and low-cost inhibitors that do not affect the quality of products deserves more extensive efforts.

The environmental friendly scale inhibitors (APELn, APECn, APEG-PG-COOH) for circulating cooling water were prepared from chloracetic acid, NaOH, allyloxy polyethoxy ether, glycidol or succinic anhydride and allylpolyethoxy carboxylate, a double-hydrophilic block copolymer. Their properties of no phosphate and nitrogen free and the (–COOH) anionic active groups[18–21] have drew tremendous attention in our previous work. However, the strong intra-molecular and intermolecular hydrogen bonds between the hydroxyl groups along the chain backbone would limit the water solubility and then lead to imperfect chelating ability even flocculation.[15,16]

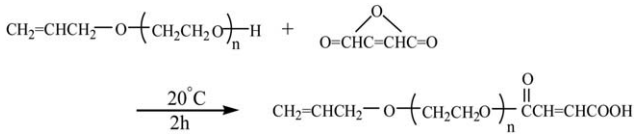

Scheme 1. Synthesis of APEY.

Due to the high electron density of oxygen atoms and high polarity, the sulfonic acid groups have strong adsorption capacity and high electrostatic repulsion, and the properties are not affected by the pH value of inhibitor medium. Therefore, a polymer containing sulfonic acid groups also play a role in the inhibition and dispersion stability in acidic environments.[22] The copolymers of scale inhibitors based on acrylic acid (AA) have been applied extensively for several decades.[23–26] AA is an anionic monomer, the most common monomer of preparing antisludging agent and rather cheap. If there were hydroxyl, amido and sulfonic acid groups in one molecule, it could enhance the solubility of scale inhibitors and bring about the increasing inhibitory capacity of the copolymer in preventing the precipitation of calcium phosphate.[17] In this study, the polymeric scale inhibition and dispersion agents (PAYS) were prepared by graft copolymerization of AA, allylpolyethoxy carboxylate (APEY), and 2-acrylamido-2-methyl-propanesulfonic acid (AMPS) by using ammonium persulfate as a radical initiator in aqueous solution. The terpolymer has different functional groups, such as carbonyl, allyloxy, amide, sulfonic acid and ester. It is reported that the adsorption capacity of ester groups is stronger than sulfonic acid groups. It can reasonably be expected that the effective nonphosphine scale inhibitor PAYS can be used to improve scaling problems.

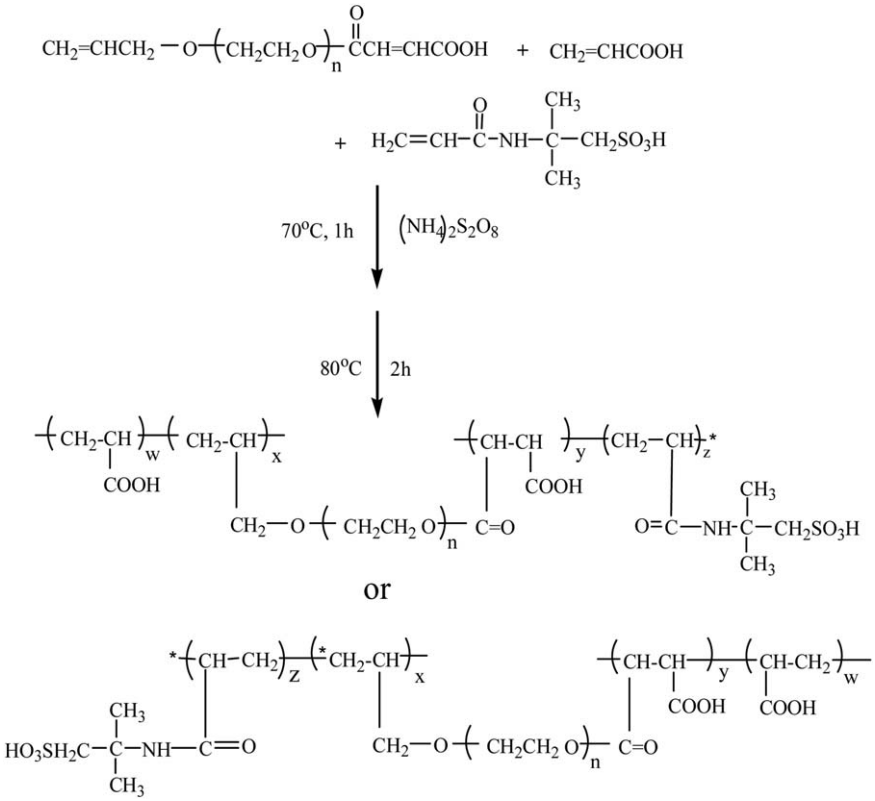

Scheme 2. Synthesis of AA/APEY/AMPS (PAYS).

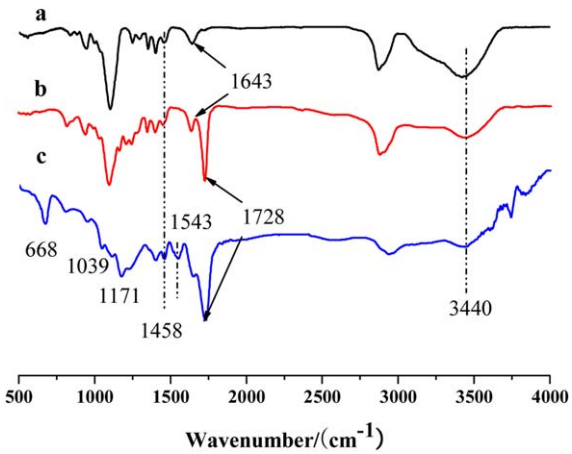

Figure 1. FT-IR spectrum of APEG (a), APEY (b), and PAYS (c). [Color figure can be viewed in the online issue, which is available at wileyonlinelibrary.com.]

EXPERIMENTAL

Materials

The allylpolyethoxy carboxylate (APEY) used in the experiment was synthesized in our laboratory according to K. Du's procedure. Maleic anhydride (MA) and AA were analytically pure grade and were supplied by Zhongdong Chemical Reagent Co., Ltd (Nanjing, China). The commercial inhibitors of poly(acrylic acid) (PAA, $M_W = 1800$), 2-phosphonobutane 1,2,4-tricarboxylic acid (PBTC, $M_W = 270$), polyepoxysuccinic acid (PESA, $M_W = 1500$), and Polyamino polyether methylene phosphonae (PAPEMP, $M_W = 600$) were technical grade and AMPS was supplied by Jiangsu Jianghai Chemical Co., Ltd. Deionized water was used throughout the experiments.

Characterization

The Fourier transform infrared spectroscopy (FT-IR) spectra were recorded for the synthesized polymer to confirm the functional groups that are responsible for the antiscaling property using a Bruker FT-IR analyzer (VECTOR-22, Bruker Co., Germany) in the pressed KBr pellets. ^{1}H-NMR spectra were taken by a Mercury VX-500 spec-trometer (Bruker AMX500) with a tetramethylsilane internal reference and deuterated dimethyl sulfoxide as the solvent. The weight distribution of the polymer was determined by gel permeation chromatography (GPC, Shodex KF-850 column) with water as the mobile phase at a flow rate 1.0 mL/min calibrated with PEG standards. The shapes of $Ca_3(PO_4)_2$ and $BaSO_4$ were observed with scanning electron microscopy (SEM; S-3400N, HITECH, Japan).

Synthesis of Antiscalant

The synthesis procedure of APEY is shown in Scheme 1. A new additive (PAYS) was prepared as following (Scheme 2) and the modified conditions were based on our preparative experiments. In brief, a 4-neck round bottom flask, equipped with a thermometer and a magnetic stirrer, was filled with 5 mL of deionized water and 2 g APEY and then heated to 70°C with stirring under nitrogen atmosphere. After that, 4 g AA and 1 g AMPS were added in 20 mL distilled water and the initiator solution (0.21 g ammonium persulfate in 20 mL distilled water) was injected into the flask separately at constant flow rates over a period of 1.0 h. After that the flask was heated to 80°C for 1.5–2.5 h with stirring. Finally, the faint yellow liquid with an approximately 25% solid content was obtained.

Static Scale Inhibition Methods

Calcium Phosphate Inhibition. All inhibitor dosages given below were on a dry-inhibitor basis. In this experiment, the effectiveness of PAYS against calcium phosphate precipitation was determined according to the national standard of PR China concerning the code for the design of industrial circulating cooling-water treatment (GB 50050-95) by the static scale inhibition test under different conditions. Supersaturated solutions of calcium phosphate for the precipitation experiment were prepared by adding a known volume of phosphate (the final PO_4^{3-} concentration would be 5 mg/L) stock solution to a glass bottle (250 mL) thermostatted at constant temperature, which contains a known volume of water. Investigation with and without inhibitors were all carried out. After temperature equilibration, the inhibitors were added before the calcium stock solution was added in such amount that the final calcium concentration would be 250 mg/L or the required values. To avoid the concentration of the solution by evaporation especially at a high temperature, we condensed the vapor by means of a cooler. Deposition of these calcium carbonate supersaturated solutions was filtered using filter paper after these solutions were incubated at 80°C for 10 h in water bath. Inhibitor efficiency as a calcium phosphate inhibitor was calculated by using the following equation:

$$\text{inihibition}(\%) = \frac{[\text{phosphate}]_{\text{final}} - [\text{phosphate}]_{\text{blank}}}{[\text{phosphate}]_{\text{initial}} - [\text{phosphate}]_{\text{blank}}} \times 100\%$$

where $[\text{phosphate}]_{\text{final}}$ = concentration of phosphate in the filtrate in the presence of inhibitors at 10 h, $[\text{phosphate}]_{\text{blank}}$ = concentration of phosphate in the filtrate in the absence of inhibitors at 10 h, and $[\text{phosphate}]_{\text{initial}}$ = concentration of phosphate at the beginning of the experiment.

Barium Sulfate Inhibition. Supersaturated solutions of barium sulfate for the precipitation experiment were according to the national standard of PR China concerning the code for the design of industrial oilfield-water treatment (SY/T 126-2005). Calcium sulfate precipitation and inhibition were studied in artificial cooling water which was prepared by dissolving a certain quantity of $BaCl_2$ and Na_2SO_4 in deionized water with $BaC1_2$ (1.40 g/L Ca^{2+}) and Na_2SO_4 (82.69 g/L SO_4^{2-}). After temperature equilibration, the inhibitors were added before the barium stock solution was added in such amount that the final barium concentration would be 28 mg/L or the required values. Precipitation in these solutions was monitored by analyzing the absorbance of solutions with UV spectrophotometer after these solutions were heated at a temperature of 50°C for 24 h. Then the absorbance is calculated as concentration of barium from working curve. The inhibition efficiency of PAYS against calcium sulfate scale was calculated by using the following equation:

$$\text{inhibition}(\%) = \frac{[\text{barium}]_{\text{final}} - [\text{barium}]_{\text{blank1}}}{[\text{barium}]_{\text{blank2}} - [\text{barium}]_{\text{blank1}}} \times 100\%$$

where $[\text{barium}]_{\text{final}}$ = concentration of barium in the filtrate in the presence of inhibitors at 10 h, $[\text{barium}]_{\text{blank1}}$ = concentration

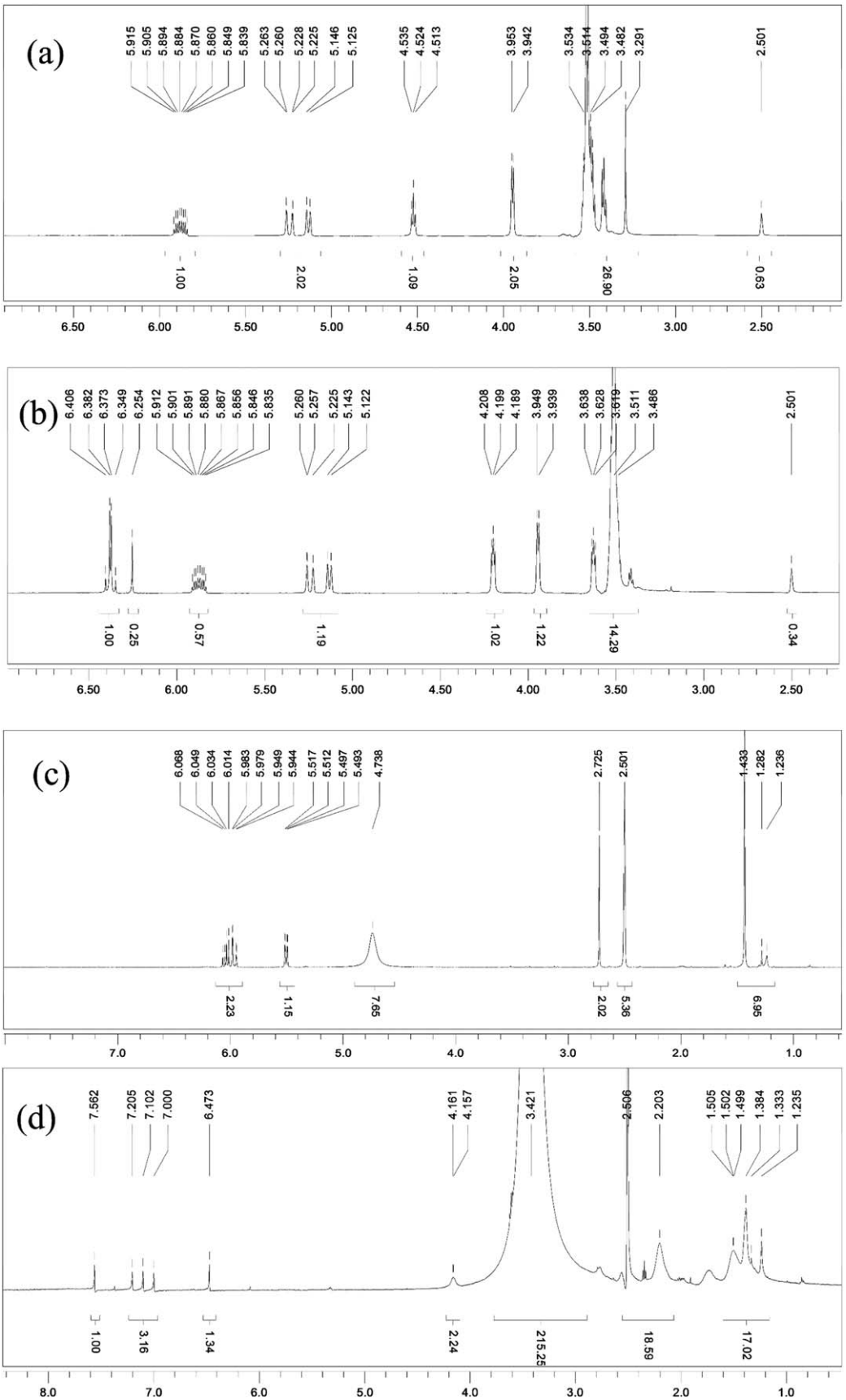

Figure 2. ^{1}H-NMR spectra of (a) APEG, (b) APEY, (c) AMPS, and (d) PAYS.

Table I. Average Molecular Weight of PAYS

AA/APEY/AMPS molar ratio	2 : 1 : 1.5	2 : 1 : 1	2 : 1 : 0.5	2 : 1.5 : 0.5	2 : 0.5 : 0.5	2 : 0.3 : 0.5
$M_w \times 10^{4a}$	1.96	1.76	1.69	1.86	1.68	1.67
$M_n \times 10^{4a}$	1.73	1.68	1.58	1.69	1.57	1.58

[a] Determined by GPC eluted with water based on PEG standards.

of barium in the filtrate in the absence of inhibitors at 10 h, and $[\text{barium}]_{\text{blank2}}$ = concentration of barium at the beginning of the experiment.

Iron (III) Inhibition. Ferrous compounds for precipitation experiments were prepared by adding a known volume of calcium stock solution to a beaker (1000 mL) at room temperature under violent stirring, with a known volume of water. After temperature equilibration, the inhibitors were added before the iron (II) (normally 5–10 mL) stock solution was added in such amount that the final iron (II) concentration would be 10 mg/L or the required values. Precipitation in these solutions was monitored by analyzing solutions for the light transmittance by using UV spectrophotometer after these solutions were heated 5 h at a temperature of 50°C. The pH 9.0 of ferrous solutions was adjusted by using dilute solutions of borax. Iron (II) ion stock solutions were prepared from iron (II) sulfate heptahydrate using de-aerated distilled water.

Polymer efficacy as iron (III) inhibitor was evaluated by using the light transmittance of ferrous solutions, which is 100% after being heated 5 h at a temperature of 50°C in the absence of inhibitor. The lower the light transmittance is, the better the polymer efficacy is as an iron (III) inhibitor.

Commercial scale inhibitors with different molecular structures and molecular weights such as PAA, PAPEMP, PESA, and PBTC were also tested to have a comparison of different inhibition efficiency.

RESULTS AND DISCUSSIONS

FT-IR Analysis of PAYS

The FT-IR spectra were taken for the synthesized PAYS and are presented in Figure 1. Functional groups are assigned for the characteristic peaks and a broad band centered near 3440 cm^{-1} is observed due to O–H stretching vibrations of hydroxyl group. The strong intensity absorption peak in the region of 1728 cm^{-1} is assigned to the stretching of –C═O group. The characteristic peak at 1643 cm^{-1} could be C═O stretching vibrations of amid group and the band at 1543 cm^{-1} is assigned to C–N stretching vibrations and N–H flexural vibrations. The peak at 1458 cm^{-1} reveals the $–CH_2$ scissoring deformation vibration. The peaks that appear at 1039 and 1171 cm^{-1} are assigned to aliphatic –S═O symmetry and asymmetry stretching vibrations of sulfonic acid groups, respectively, and the S–O stretching peaks at 668 cm^{-1}.[20,27] The expected structure and the functional groups, which are responsible for the inhibiting character of the PAYS, are primarily confirmed. Compared to the FT-IR spectra of APEG, APEY, and PAYS, the appeared peak at 1728 cm^{-1} in Figure 1(b) and double bond absorption peaks disappearing in Figure 1(c), all of these changes also suggest that APEY and PAYS were synthesized successfully.

^{1}H-NMR Analysis of PAYS

The ^{1}H-NMR spectra of APEG, APEY, AMPS, and PAYS are presented in Figure 2. The ^{1}H-NMR data were acquired as the following and the chemical molecule structures were deduced as expected.

APEG(a) [$(CD_3)_2SO$, δ ppm]: 2.50 [solvent residual peak of $(CD_3)_2SO$], 3.29–3.53 ($–OCH_2CH_2–$, ether group), 3.94 (CH_2═$CH–CH_2–$, propenyl protons), 4.51–4.54 (–OH, active hydrogen in APEG), and 5.12–5.92 (CH_2═$CH–CH_2–$, propenyl protons).

APEY(b) [$(CD_3)_2SO$, δ ppm]: 2.50 [solvent residual peak of $(CD_3)_2SO$], 3.49–3.84 ($–OCH_2CH_2–$, ether group), 3.94 (CH_2═$CH–CH_2–$, propenyl protons), 4.2 (–CH═CH–, ethylene protons), 5.12–5.91 (CH_2═$CH–CH_2–$, propenyl protons), and 6.25–6.41 (–CH═CH–, ethylene protons).

AMPS(c) [$(CD_3)_2SO$, δ ppm]: 2.50 [solvent residual peak of $(CD_3)_2SO$], 1.24–1.43 ($–CH_3$, methyl proton), 2.73 (–CONH–, acylamino), 4.74 ($–CH_2–$, methylene protons), and 5.49–6.07 (CH_2═$CH–$, ethylene protons).

PAYS(d) [$(CD_3)_2SO$, δ ppm]: 2.50 [solvent residual peak of $(CD_3)_2SO$], 1.23–1.75 ($–CH_3$, methyl proton), 2.20 (–CONH–, acylamino), 3.42 ($-OCH_2CH_2-$, ether group), and 4.15 ($–CH_2–$, methylene protons).

Table II. Influence of the Dosage and Mole Ratio of PAYS on the Inhibition Tests of $Ca_3(PO_4)_2$

Dosage of inhibitor (ppm)	2 : 1 : 1.5	2 : 1 : 1	2 : 1 : 0.5	2 : 1.5 : 0.5	2 : 0.5 : 0.5	2 : 0.3 : 0.5
2	27.8%	23.1%	19.0%	35.2%	32.0%	32.1%
4	66.8%	78.3%	70%	75.1%	72.4%	77.4%
6	94.5%	100%	98.5%	96.2%	95.1%	98.7%
8	99.8%	100%	100%	100%	99.7%	99.8%
10	100%	100%	100%	99.9%	100%	100%
12	100%	99.8%	99.9%	100%	100%	100%

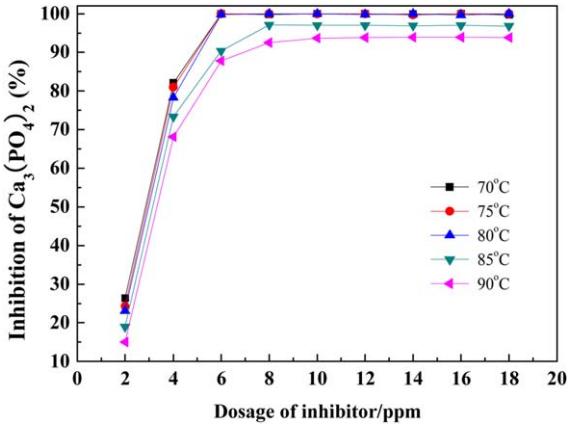

Figure 3. Scale inhibition of AA/APEY/AMPS at different temperature on $Ca_3(PO_4)_2$. [Color figure can be viewed in the online issue, which is available at wileyonlinelibrary.com.]

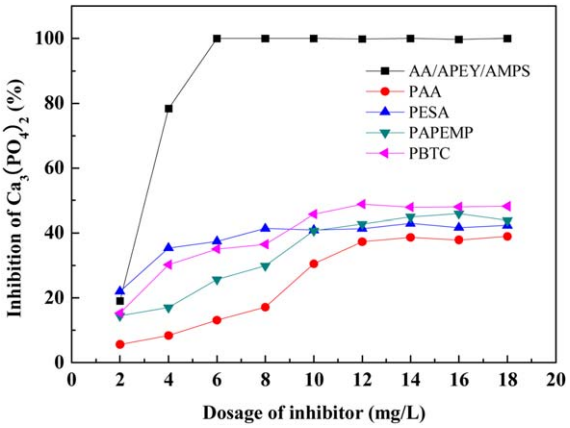

Figure 5. Scale inhibition of AA/APEY/AMPS and different commercial inhibitor on $Ca_3(PO_4)_2$ at different concentrations, respectively. [Color figure can be viewed in the online issue, which is available at wileyonlinelibrary.com.]

The disappeared peak at 4.51–4.54 ppm (–OH) and appeared peak at 4.2, 6.25–6.41 ppm (–CH═CH–) in Figure 2(b) demonstrates that active hydroxyl group in APEG has reacted with MA. Meanwhile, it was obvious that the double bond absorption peaks ($\delta = 5.12$–5.91, 5.49–6.07, 4.2, and 6.25–6.41 ppm) disappeared completely, all of these data further suggest that PAYS was synthesized successfully.

GPC Analysis of PAYS

The weight distribution of the polymer PAYS was investigated with GPC at the 1.0 mL/min run flow rate and the results were presented in Table I. We found the mass-average molecular weight (Mw) spread between the interval of $1.67 \times 10^4 \sim 1.96 \times 10^4$ whereas the number-average molecular weight (Mn) ranged from 1.57×10^4 to 1.73×10^4.

Effect of PAYS on $Ca_3(PO_4)_2$ Scale

For the data in Table II, the properties of PAYS prepared at different AA: APEY: AMPS mole ratio are summarized and we have determined that antiscalant concentration and mole ratio greatly influence the performance of terpolymer PAYS. Thus, as the concentration of these trimers increase, their protection effect and the scale inhibition efficiency increase. It was obvious that PAYS has an efficiency of 100% for $Ca_3(PO_4)_2$ at 10 mg/L. The different molar ratio of PAYS resulted in different inhibition capacity toward $Ca_3(PO_4)_2$ scales, and the threshold (critical value) was changed but reached a maximum value of 100% finally when the dosage was only 8 ppm. The copolymer molecular chain contains carboxylate (–COOH), carboxamide (–CONH), and sulfonate (–SO_3H) groups which have positive dispersion, excellent chelation, superior compatibilization with Ca^{2+} ion and lattice distortion ability. These active functional groups possess good properties for Ca scale. For the same scale inhibitor, as the concentration gradually increased, the interaction between the scale inhibitor and Ca^{2+} ion became increasingly stronger, and the scale inhibitive performance of the polymer also improved. Tab.I manifests that PAYS (AA: APEY: AMPS = 2 : 1 : 1, mole ratio) show superior efficiency in $Ca_3(PO_4)_2$ inhibition than other mole ratio at the same concentration of PAYS.

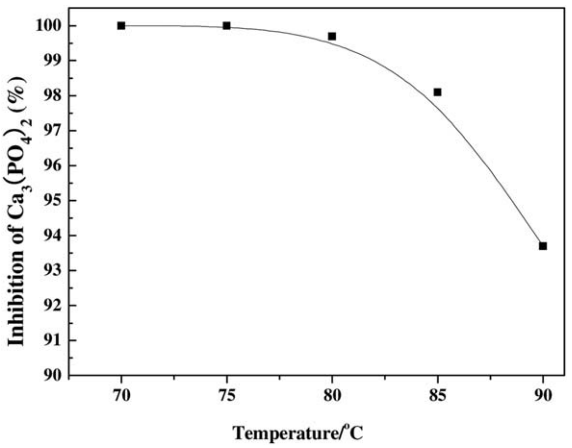

Figure 4. Temperature on scale inhibition of AA/APEY/AMPS on $Ca_3(PO_4)_2$.

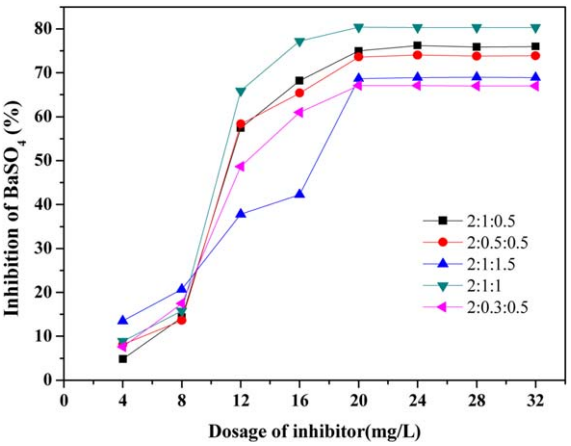

Figure 6. Scale inhibition of AA/APEY/AMPS (different mole ratio) on $BaSO_4$ at different concentrations of copolymers, respectively. [Color figure can be viewed in the online issue, which is available at wileyonlinelibrary.com.]

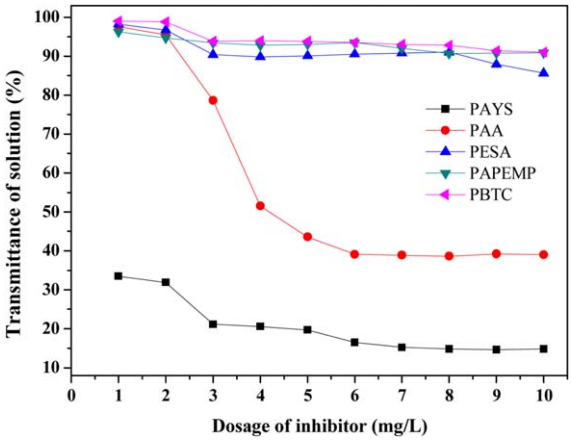

Figure 7. Iron hydroxide dispersion of AA/APEY/AMPS and different commercial inhibitor at different concentrations. [Color figure can be viewed in the online issue, which is available at wileyonlinelibrary.com.]

Influence of Temperature on $Ca_3(PO_4)_2$ Inhibition

From the above results, the molar ratio of the best anti scale effects to calcium phosphate is 2 : 1 : 1, and temperature effect on testing the terpolymer efficiency was investigated. As shown in Figure 3, the scale inhibition efficiency increased with increasing concentration of the PAYS. Meanwhile, the primary efficiency and threshold concentration existed distinctive differences. The results in Figure 4 were examined under magnification and there appears to be a rise in the growth rate at a critical supersaturation as the temperature increases, which means the inhibition capacity has gone off. When temperature increased to 90°C, the maximum inhibition efficiency dropped to 93.7% but it still exceeded 90%. The reaction was so vigorously at high temperature that it was difficult to control and high temperature also caused the reaction rate increased, the molecular weight of terpolymer compounds decreased and the inhibition efficiency weaken.

Comparisons of $Ca_3(PO_4)_2$ Inhibition Efficiency

Compared to low-phosphorus and nonphosphorus polymers, such as PAA, PESA, PAPEMP and PBTC, the antisludging agent AA/APEY/AMPS exhibited improved or excellent properties anti-$Ca_3(PO_4)_2$. It is worth mentioning that the threshold dosage is 6 mg/L for PAYS, whereas the commercial scale inhibitors have a disadvantage in the threshold dosage and it is 10 mg/L. As shown in Figure 5, AA/APEY/AMPS has superior ability to control $Ca_3(PO_4)_2$ deposits, with 100% inhibition at a level of 6 mg/L. However, it is 13.2% for PAA at the same dosage, at which PESA has only 37.5% calcium phosphate inhibition, 25.7% for PAPEMP and 35.2% for PBTC, which is in accordance with the results of supposed. It is indicated that the capacity of preventing the precipitation of Ca^{2+} from bulk solution is PAYS > PBTC > PAPEMP > PESA > PAA. These inhibitors containing carboxyl groups like AA/APEY/AMPS, especially PAA possesses molecular structure like to the terpolymer, but it can hardly prevent the precipitation of $Ca_3(PO_4)_2$ even at a high dosage. One reason may be the side-chain polyethylene segments of APEY together with carboxyl groups of AA during the process of control $Ca_3(PO_4)_2$ scales. It can be concluded that the scale inhibitor synthesized PAYS is a potentially effective green alternative in inhibiting $Ca_3(PO_4)_2$ scales.

Effect of Inhibitor on Barium Scale

To evaluate the efficacy of terpolymer as $BaSO_4$ deposits inhibitor, a series of precipitation experiments were implemented at varying concentrations of terpolymer. In Figure 6, we plot the changes in percent inhibition values for barium sulfate. The results showed that the inhibition efficiency of barium sulfate tends to increase as the concentration of PAYS increased and the effects depend on mole ratio of AA/APEY/AMPS. At the same concentration of PAYS, the $BaSO_4$ scale inhibition efficiency value was observed to decrease in the order: 2 : 1 : 1 (AA: APEY: AMPS, mole ratio) > 2 : 1 : 0.5 > 2 : 0.5 : 0.5 > 2 : 0.3 : 0.5 > 2 : 1 : 1.5. It is also clear that PAYS exhibits an obvious "threshold effect" and the maximum calcium tolerance is 80% $BaSO_4$ inhibition efficiencies at the dosage of 20 mg/L. It is observed that commercial inhibitors, PAA, PBTC and PESA, were also tested at same experimental conditions and these inhibitors almost have any

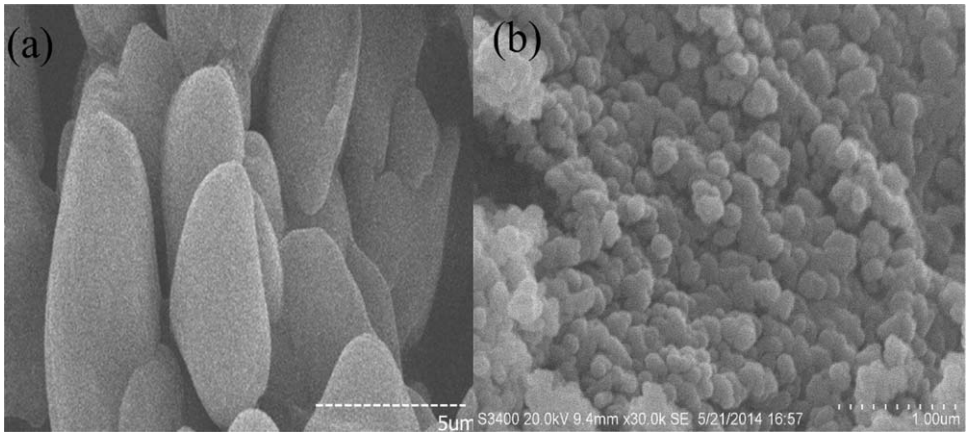

Figure 8. SEM images of $Ca_3(PO_4)_2$ crystals: (a) in the absence of AA/APEY/AMPS; (b) in the presence of 4 mg/L AA/APEY/AMPS.

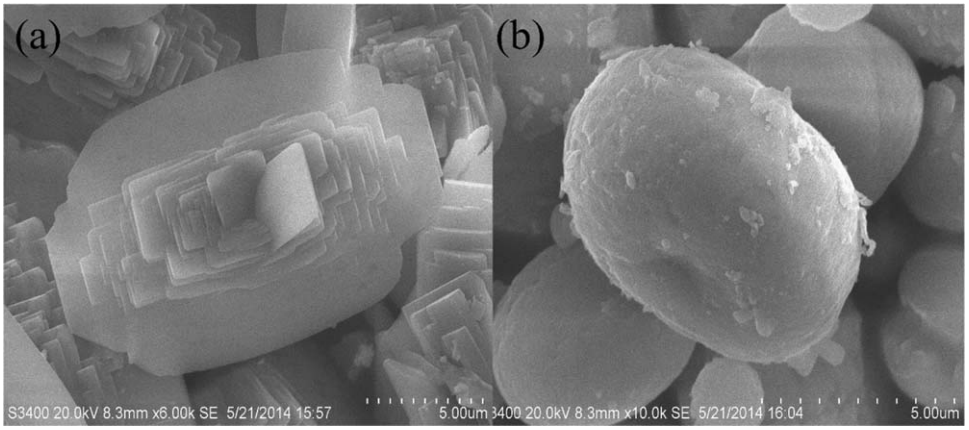

Figure 9. SEM images of $BaSO_4$ crystals: (a) in the absence of AA/APEY/AMPS; (b) in the presence of 15 mg/L AA/APEY/AMPS.

leverage but PESA have the maximum efficiency 65% at the dosage of 30 mg/L.

Effect of Inhibitor on Iron (III) Dispersion

The terpolymer PAYS has excellent dispersion as iron dispersing agent, which was examined in the presence of varying concentrations of PAYS together with commercial inhibiters and the data is shown in Figure 7. The dispersion efficiency is the reciprocal of transmission, in other words, the lower of transmission, the better of effect on iron dispersion. The results indicated that the dosage affecting the capacity of control iron (III) precipitation is just not strongly besides PAA. The transmittance of the iron (III) solution was 33.5% in the presence of PAYS at a level of 1 mg/L, whereas other commercial inhibitors have not worked yet at the same dosage. It is worth mentioning that the threshold dosage of PAYS in consonance with PAA is 6 mg/L, other inhibitors have advantage threshold dosage only at 3 mg/L, but they provide only nearly 85% transmission. PAYS possesses preeminent dispersive ability for iron scale compared to commercial inhibitors reported above and prevents equipment corrosion caused by iron (III) precipitation.

Characterization of Scales

For the sake of analyzing the influence of AA/APEY/AMPS on the growth of $Ca_3(PO_4)_2$ crystal, $Ca_3(PO_4)_2$ scales were collected according to the experimental method on the condition of the appropriate concentration. Figure 8 shows the SEM images of $Ca_3(PO_4)_2$ scale particles obtained in the absence and presence of AA/APEY/AMPS.

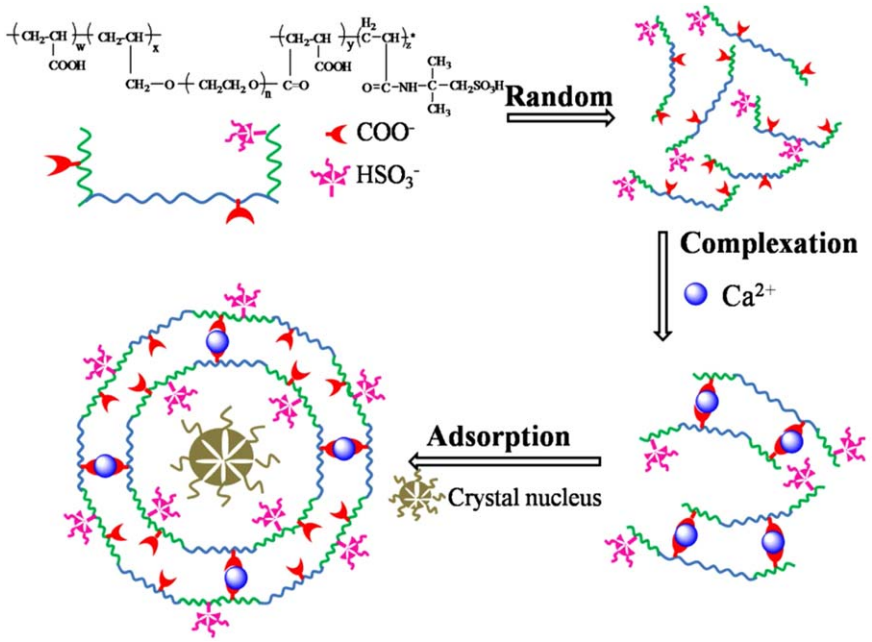

Figure 10. Schematic diagrams of AA/APEY/AMPS inhibition on calcium scales: chelating solubilization and adsorption. [Color figure can be viewed in the online issue, which is available at wileyonlinelibrary.com.]

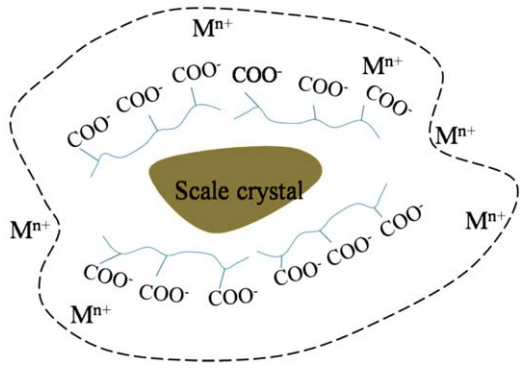

Figure 11. The adsorption of terpolymer scale inhibitor on surface of scale crystal. [Color figure can be viewed in the online issue, which is available at wileyonlinelibrary.com.]

The SEM image [Figure 8(a)] revealed that the $Ca_3(PO_4)_2$ crystals precipitated from supersaturated calcium orthophosphate solution in the absence of inhibitor exhibited mainly regular grain-shaped particles with average particle size about 8 μm. However, with addition of 4 ppm of the inhibitor, it has obvious changes at the distribution and size as shown in Figure 8(b). Crystals grown were smaller in size about 0.2 μm and the particles loosened to be easily washed away by a fluid. Therefore, it is possible to assume that the carboxylic acid groups bind multivalent cation with powerful affinities and possess excellent chelate ability, –COOH group of PAYS complexes with Ca^{2+} could form soluble. These changes indicate that the terpolymer has great influence on the nucleation and crystallization of the $CaCO_3$ precipitate.

The changes in $BaSO_4$ crystal habit, size and modifications, brought about by the PAYS polymer addition, were also tested through transmission electron microscopy. High resolution SEM images of barium sulfate with the absence and the presence of the polymer PAYS are presented in Figure 9(a,b), respectively.

In the absence of inhibitor [Figure 9(a)], barium sulfate particles are olive-shaped and interstall pillar plane is the largest, approximately 12–13 μm and covering toward two sides layer by layer. When the terpolymer PAYS is added, barium sulfate particles exhibit persimmon shaped with average particle size about 5 μm. The substantial differences in morphology and size clearly confirm that there are differences in the interactions with the forming crystal nucleus and growing crystal surface. It is possible that the ester groups of APEY and sulfonic acid groups (–SO_3H) of AMPS adsorb on the $BaSO_4$ crystal nucleus, hindering the growth of active sites. The incorporation of AA/APEY/MPSA results in the crystal interfacial tension increases and thus blocks further precipitation.[17] The results suggest that PAYS affect the morphological changes in scales greatly and block crystal growth as typical $BaSO_4$ inhibitors.[28]

The Mechanism of Scale Inhibition

The results reported above maybe provide a hypothetical mechanism of the scale inhibition, as depicted in Figure 10 (Ca scale as an example). The scale inhibition process of insoluble salt can be divided into two steps roughly, generation of crystal nucleus and the growth of scale forming salt crystallites.[29] It is generally accepted that the carboxylic acid groups could bind multivalent cation ($M^{n+} = Ca^{2+}$, Ba^{2+}, Fe^{3+}, etc.) via excellent chelating ability and powerful affinities. So PAYS could form soluble complexes with M^{n+} through –COOH.[30–32] The phenomenon could reduce the free M^{n+} concentrations, decrease the supersaturation and block the growth of active sites. The rate of hydrophilic chain segment in the polymer chain also affects the interaction with the scale deposit nuclei forming. Increasing the ratio of AA leads to the hydrophilic chain grew in length, thus the comb structure of polymer grew and steric hindrance enhanced, thereby decreasing the rate of crystal nucleus formation. PAYS can strongly adsorb onto a $CaCO_3$ crystalline substrate owing to –COO– of APEY segment and –SO_3H interaction with electric charge in the surface of crystal nucleus, disturbing and slow-downing the crystal growth due to the adsorption of the polymeric species maybe at the active sites of crystal nucleus.[1] Otherwise, the –SO_3H groups strengthened polymer solubility and then improved extension of the molecular chain, and the molecular chain encapsulate crystal nucleus more easily and steadily.[20] Consequently, due to –COO– adsorption, the electrostatic effect can lead to macromolecule chains and crystal nucleus with lots of anionic charge and forming electric double layer, as shown in Figure 11. Two like electric charges repel each other, preventing collisions between them and blocking the formation of large crystals. Meanwhile, these polymers function groups, such as –COOH, –CONHR, –SO_3H, –COOR, by adsorbing on to iron oxide particles, prevent iron (III) from settling on the equipment surfaces and disperse on circulating water system.[1]

CONCLUSIONS

The polymeric scale inhibition and dispersion agents (PAYS) were prepared by graft copolymerization of AA, allylpolyethoxy carboxylate (APEY, prepared in our laboratory before) and AMPS by using ammonium persulfate as a radical initiator in aqueous solution, and the structure was characterized by FT-IR. The result showed that the terpolymer molecular chain comprises carbonyl, allyloxy, amide, sulfonic acid, and ester. As demonstrated in this study, considerable performance benefits can be realized simply in static scale inhibition experiments for $Ca_3(PO_4)_2$ and $BaSO_4$. The results of the present study are summarized as follows:

1. The AA/APEY/AMPS had an excellent efficiency of scale inhibition, and the maximum inhibition efficiency reached 100% when the dosage was only 6 ppm vastly superior to the scale inhibitor on the market in our experiments.
2. PAYS was also an effective $CaSO_4$ inhibitor under condition of pH = 7, and about 20 ppm combination of PAYS provided almost 80% inhibition efficiency while PAA and other excellent scale inhibitors had any leverage anymore.
3. PAYS possessing preeminent dispersive ability for iron scale compared to commercial inhibitors reported above and the transmittance of the iron (III) solution was 33.5% at a level of 1 mg/L PAYS.

Characterization of $Ca_3(PO_4)_2$ and $BaSO_4$ scales was examined by SEM, the scanning electron micrographs revealed that

obvious change at the distribution, size and morphology of scales occurred under the effect of PAYS. In addition, the terpolymer had excellent dispersing ability to iron (III). These results indicate that PAYS is a potentially effective green alternative in inhibiting scales for circulating cooling water.

ACKNOWLEDGMENTS

This work was supported by the Prospective Joint Research Project of Jiangsu Province (BY2012196); the National Natural Science Foundation of China (51077013); Special funds for Jiangsu Province Scientific and Technological Achievements Projects of China (BA2011086); Program for Training of 333 High-Level Talent, Jiangsu Province of China (BRA2010033); and Scientific Innovation Research Foundation of College Graduate in Jiangsu Province (CXLX13-107).

REFERENCES

1. Amjad, Z.; Koutsoukos, P. G. *Desalination* **2014**, *335*, 55.
2. Zhang, H.; Wang, F.; Jin, X.; Zhu, Y. C. *Desalination* **2013**, *326*, 55.
3. Du, K.; Zhou, Y. M.; Wang, L. Q.; Wang, Y. Y. *J. Appl. Polym. Sci.* **2009**, *113*, 1966.
4. Mahgoub, F. M.; Abdel-Nabey, B. A.; El-Samadisy, Y. A. *Mater. Chem. Phys.* **2010**, *120*, 104.
5. Cao, K.; Zhou, Y. M.; Liu, G. Q.; Wang, H. C.; Sun, W. *J. Appl. Polym. Sci.* **2014**, DOI: 10.1002/APP.40193.
6. Jing, G.; Li, X. *Res. J. Appl. Sci. Eng. Technol.* **2013**, *6*, 3472.
7. Kavitha, A. L.; Vasudevan, T.; Prabu, H. G. *Desalination* **2011**, *268*, 38.
8. Shakkthivel, P.; Vasudevan, T. *J. Appl. Polym. Sci.* **2007**, *103*, 3206.
9. Koutsopoulos, S.; Dalas, E. *J. Colloid Interface Sci.* **2000**, *231*, 207.
10. Brinis, H.; Samar, M. E. H. *Desal. Wat. Treat.* **2012**, *44*, 190.
11. Kumar, T.; Vishwanatham, S.; Kundu, S. S. *J. Petrol. Sci. Eng.* **2010**, *71*, 1.
12. Bahri, S.; Endaryanto, T. *Desalination* **2011**, *265*, 102.
13. Al Nasser, W. N.; Al-Salhi, F. H.; Hounslow, M. J.; Salman, A. D. *Chem. Eng. Res. Des.* **2011**, *89*, 500.
14. Hasson, D.; Shemer, H.; Sher, A. *Ind. Eng. Chem. Res.* **2011**, *50*, 7601.
15. Wang, C.; Zhu, D. Y.; Wang, X. K. *J. Appl. Polym. Sci.* **2010**, *115*, 2149.
16. Bao, Y.; Ma, J.; Li, N. *Carbohydr. Polym.* **2011**, *84*, 76.
17. Yin, X. SH.; Yang, W. ZH.; Tang, Y. G. *Desalination* **2010**, *255*, 143.
18. Liu, G. Q.; Huang, J. Y.; Zhou, Y. M.; Yao, Q. Z.; Ling, L.; Zhang, P. X.; Wang, H. C.; Cao, K.; Liu, Y. H.; Wu, W. D.; Sun, W. *Tenside Surf. Det.* **2012**, *5*, 404.
19. Fu, C. E.; Zhou, Y. M.; Huang, J. Y.; Xie, H.; Liu, G. Q.; Wu, W. D.; Sun, W. *Tenside Surf. Det.* **2011**, *48*, 60.
20. Liu, G. Q.; Huang, J. Y.; Zhou, Y. M.; Yao, Q. Z.; Ling, L.; Zhang, P. X.; Fu, C. E.; Wu, W. D.; Sun, W.; Hu, Z. *J. Tenside Surf. Det.* **2012**, *3*, 216.
21. Fu, C. E.; Zhou, Y. M.; Liu, G. Q.; Huang, J. Y.; Sun, W.; Wu, W. D. *Ind. Eng. Chem. Res.* **2011**, *50*, 10393.
22. Baklouti, S.; Romdhane, M. R. B.; Boufi, S. *J. Eur. Ceram. Soc.* **2003**, *203*, 905.
23. Shakkthivel, P.; Vasudevan, T. *Desalination* **2006**, *197*, 179.
24. Choi, D. J.; You, S. J.; Kim, J. G. *Mater. Sci. Eng.* **2002**, *35*, 228.
25. Butt, F. H.; Rahman, F.; Baduruthamal, U. *Desalination* **1997**, *109*, 323.
26. Gill, J. S.; Varsanik, R. G. *J. Cryst Growth* **1986**, *76*, 57.
27. Lin, S. B.; Yuan, C. H.; Ke, A. R.; Quan, Z. L. *Sens. Actuators B: Chem.* **2008**, *134*, 281.
28. Bunney, K.; Freeman, S.; Ogden, M. I. *Cryst. Growth. Des.* **2014**, *14*, 1650.
29. Liu, G. Q.; Huang, J. Y.; Zhou, Y. M.; Yao, Q. Z.; Ling, L.; Zhang, P. X.; Fu, C. E.; Wu, W. D.; Sun, W. *Tenside Surf. Det.* **2012**, *49*, 216.
30. Wang, C.; Li, S. P.; Li, T. D. *Desalination* **2009**, *249*, 1.
31. Demadis, K. D.; Katarachia, S. D. *Phosphorus, Sulfur Silicon Relat. Elem.* **2004**, *179*, 627.
32. Liu, H. ZH.; Schonberger, K. D.; Peng, CH. Y. *Water Res.* **2013**, *47*, 3817.